

RESEARCH

Open Access



# Sex and interspecies differences in ESR2-expressing cell distributions in mouse and rat brains

Masahiro Morishita<sup>1</sup>, Shimpei Higo<sup>1</sup>, Kinuyo Iwata<sup>1</sup> and Hirotaka Ishii<sup>1\*</sup> 

## Abstract

**Background** ESR2, a nuclear estrogen receptor also known as estrogen receptor  $\beta$ , is expressed in the brain and contributes to the actions of estrogen in various physiological phenomena. However, its expression profiles in the brain have long been debated because of difficulties in detecting ESR2-expressing cells. In the present study, we aimed to determine the distribution of ESR2 in rodent brains, as well as its sex and interspecies differences, using immunohistochemical detection with a well-validated anti-ESR2 antibody (PPZ0506).

**Methods** To determine the expression profiles of ESR2 protein in rodent brains, whole brain sections from mice and rats of both sexes were subjected to immunostaining for ESR2. In addition, to evaluate the effects of circulating estrogen on ESR2 expression profiles, ovariectomized female mice and rats were treated with low or high doses of estrogen, and the resulting numbers of ESR2-immunopositive cells were analyzed. Welch's t-test was used for comparisons between two groups for sex differences, and one-way analysis of variance followed by the Tukey–Kramer test were used for comparisons among multiple groups with different estrogen treatments.

**Results** ESR2-immunopositive cells were observed in several subregions of mouse and rat brains, including the pre-optic area, extended amygdala, hypothalamus, mesencephalon, and cerebral cortex. Their distribution profiles exhibited sex and interspecies differences. In addition, low-dose estrogen treatment in ovariectomized female mice and rats tended to increase the numbers of ESR2-immunopositive cells, whereas high-dose estrogen treatment tended to decrease these numbers.

**Conclusions** Immunohistochemistry using the well-validated PPZ0506 antibody revealed a more localized expression of ESR2 protein in rodent brains than has previously been reported. Furthermore, there were marked sex and interspecies differences in its distribution. Our histological analyses also revealed estrogen-dependent changes in ESR2 expression levels in female brains. These findings will be helpful for understanding the ESR2-mediated actions of estrogen in the brain.

\*Correspondence:

Hirotaka Ishii

hirotaka@nms.ac.jp

Full list of author information is available at the end of the article



© The Author(s) 2023. **Open Access** This article is licensed under a Creative Commons Attribution 4.0 International License, which permits use, sharing, adaptation, distribution and reproduction in any medium or format, as long as you give appropriate credit to the original author(s) and the source, provide a link to the Creative Commons licence, and indicate if changes were made. The images or other third party material in this article are included in the article's Creative Commons licence, unless indicated otherwise in a credit line to the material. If material is not included in the article's Creative Commons licence and your intended use is not permitted by statutory regulation or exceeds the permitted use, you will need to obtain permission directly from the copyright holder. To view a copy of this licence, visit <http://creativecommons.org/licenses/by/4.0/>. The Creative Commons Public Domain Dedication waiver (<http://creativecommons.org/publicdomain/zero/1.0/>) applies to the data made available in this article, unless otherwise stated in a credit line to the data.

## Highlights

- Immunohistochemical analyses using a well-validated antibody revealed that ESR2 is localized to subregions of the preoptic area, extended amygdala, hypothalamus, mesencephalon, and cerebral cortex in mouse and rat brains.
- Sex and interspecies differences in ESR2 expression were observed in some brain subregions.
- Circulating estrogen levels affected ESR2 expression in the brains of female mice and rats.

**Keywords** Mouse, Rat, Brain, Estrogen, ESR2, ER $\beta$ , Immunohistochemistry, Sexual dimorphism, Species difference

## Plain Language Summary

Although the brain is a major target organ of estrogens, the distribution of estrogen receptors in the brain is not fully understood. ESR2, also known as estrogen receptor  $\beta$ , is an estrogen receptor subtype; its localization in the brain has long been controversial because it has traditionally been difficult to detect. In the present study, we analyzed the expression sites of ESR2 in mouse and rat brains using immunohistochemistry with a well-validated antibody, PPZ0506. The immunohistochemical analysis revealed a more localized expression of ESR2 protein in brain subregions than has previously been reported. Additionally, there were clear sex and interspecies differences in the distribution of this protein. We also observed changes in ESR2 expression in the female brain in response to circulating estrogen levels. Our results, which show the precise expression profiles of ESR2 protein in rodent brains, will be helpful for understanding the ESR2-mediated actions of estrogen.

## Background

Estrogen receptors are expressed in various brain regions and regulate both reproductive and non-reproductive processes in both sexes. Two types of nuclear receptor isoforms, ESR1 and ESR2 (also known as estrogen receptor  $\alpha$  and  $\beta$ , respectively), play critical roles in estrogenic actions [1, 2]. Studies using gene knockout models and selective agonists have shown that each estrogen receptor is involved in distinct developmental and physiological events. In rodents, ESR1 is essential for sexual differentiation of the brain during development [3] as well as for the regulation of reproductive neuroendocrine function [4, 5], energy metabolism [6, 7], and social behaviors [8, 9] in adulthood; it is expressed in brain regions involved in these developmental and physiological processes. ESR2 has been implicated in several physiological processes, including reproductive neuroendocrine function [10], social behaviors [8, 11], learning and memory [12], and anxiety [13]. However, despite the importance of these phenomena, the neural mechanisms of the ESR2-mediated actions of estrogen are not well understood, largely because of the difficulties in detecting ESR2-expressing cells.

Several factors, including sex, age, and physiological conditions, can influence the actions of estrogen. Its actions presumably depend on the hormonal milieu as well as the expression levels of estrogen receptors at target sites. ESR1 is expressed in sexually dimorphic patterns in many brain regions, such as the preoptic area, bed nucleus of the stria terminalis (BNST), ventromedial

hypothalamic nucleus, arcuate nucleus, and amygdala; its expression levels are markedly altered by blood estrogen levels [14, 15]. Expression of ESR2 may also be differentially regulated under various physiological conditions. In the preoptic area of female rats, for example, *ESR2* and *ESR1* mRNA levels are elevated in the diestrus and estrus phases, respectively [16]. The expression profiles of *ESR1* and *ESR2* are thus differentially regulated at mRNA levels by different hormonal environments.

Several attempts have been made to examine the distributions of ESR2-expressing cells in rodent brains using homemade and commercial antibodies; such studies have revealed that ESR1 and ESR2 exhibit different expression patterns [17–21]. For example, it has been consistently reported that ESR2 is abundantly expressed in the hypothalamic paraventricular nucleus (PVN), whereas ESR1 is absent. However, several discrepancies have been reported in ESR2 expression in other brain regions, probably because of differences in antibody specificity. Although other approaches have been attempted, such as in situ hybridization for *ERS2* mRNA [22, 23] or the generation of transgenic mice expressing fluorescent proteins under *ESR2* promoter [24–26], these techniques are unable to directly detect ESR2 protein. The lack of validated tools to detect ESR2 had led to a halt in ESR2 research. Recently, however, a report by Anderson et al. [27] has overcome this problem. These authors evaluated the specificity of commercially available antibodies against human ESR2 and identified just one anti-human ESR2 monoclonal antibody (PPZ0506) with specific

immunoreactivity against human ESR2 protein. To further validate this antibody for use in ESR2 research, we confirmed its specificity and cross-reactivity against mouse and rat ESR2 and optimized its protocols for immunohistological analysis [28–30]. These studies revealed species-related differences in ESR2 expression in the peripheral tissues of mice and rats [29, 30]. However, although the brain is a primary target site of estrogen, the precise expression profiles of ESR2 in the brain remain unclear. In the present study, we aimed to identify sex and interspecies differences in ESR2 distributions in rodent brains by mapping ESR2-immunopositive (ESR2<sup>+</sup>) cells in the whole brains of mice and rats of both sexes. Furthermore, we examined the effects of estrogen manipulations on ESR2<sup>+</sup> cell numbers in brain subregions of female mice and rats.

## Materials and methods

### Animals

We used sexually naïve 9- to 16-week-old C57BL/6J mice and Wistar rats of both sexes. The animals were housed on a 14-h light/10-h dark cycle (lights on at 8:00 a.m.) at room temperature (22 °C ± 2 °C) with free access to a standard diet and tap water.

### Experimental design

#### *Mapping of ESR2<sup>+</sup> cells in mice and rat brains*

Gonadally intact male mice (n=4) and rats (n=4) were euthanized and histologically processed. Gonadally intact female mice (n=4) and rats (n=4) were monitored for their estrous cycles by daily vaginal smear cytology. After the confirmation of two regular estrous cycles, they were euthanized in the diestrus phase for histological processing. One series of whole brain sections from the individual animals underwent immunohistochemistry for ESR2 and Nissl staining, to examine ESR2<sup>+</sup> cell distribution. In addition, ESR2<sup>+</sup> cell numbers were counted in the neural nuclei in which ESR2 proteins were predominantly localized. Other series of the brain sections underwent double immunohistochemistry for ESR2/oxytocin (OXT) and ESR2/arginine vasopressin (AVP).

#### *Effects of estrogen manipulation on the distribution and number of ESR2<sup>+</sup> cells*

After the confirmation of two regular estrous cycles by daily vaginal smear cytology, female mice (n=15) and rats (n=15) were randomized into three groups: ovariectomy+vehicle treatment (control; n=5 for each species), ovariectomy+low-dose estrogen treatment (low-E; n=5 for each species), and ovariectomy+high-dose estrogen treatment (high-E; n=5 for each species). All female mice and rats were anesthetized by inhalation of isoflurane gas (concentration, 1%–3% in the air; flow

rate, 0.5 L/min), ovariectomized, and implanted subcutaneously with a silicon tube, which was filled with different concentrations of estrogens for each experimental group (see Fig. 1A for the time-course details). For mice, the implanted silicon tube (inner diameter 1.02 mm, outer diameter 2.16 mm, length 18.0 mm, length of tube filled with substance 12.0 mm; Dow Corning Corporation, Midland, MI, USA) was filled with sesame oil for the control, 0.1 µg/µL 17β-estradiol (E<sub>2</sub>) in sesame oil for the low-E group, or 0.2 µg/µL E<sub>2</sub> in sesame oil for the high-E group. For rats, the implanted silicon tube (inner diameter 1.57 mm, outer diameter 3.18 mm, length 37.0 mm, length of tube filled with substance 25.0 mm for the control and low-E groups; inner diameter 1.02 mm, outer diameter 2.16 mm, length 32.0 mm, length of tube filled with substance 20.0 mm for the high-E group; Dow Corning Corporation) was filled with either sesame oil for the control, 0.2 µg/µL E<sub>2</sub> in sesame oil for the low-E group, or crystalline E<sub>2</sub> for the high-E group. The ends of the substance-filled silicon tubes were sealed with glue (length of glue at each end: 3 mm for mice and 6 mm for rats). Six days after surgery, high-E mice were injected subcutaneously with estradiol benzoate in sesame oil (1 µg/100 µL) 3 h after light onset in the light/dark cycle. We euthanized the control mice and rats 14 days after surgery, the low-E mice and rats and high-E mice 7 days after surgery, and the high-E rats 2 days after surgery. The conditions for estrogen manipulation and brain sampling were set according to commonly used methods, with low-E treatment used to mimic estrogen levels within the physiological range that produce a negative feedback effect on luteinizing hormone pulses [31, 32], and high-E treatment leading to excessive estrogen levels that produce a positive feedback effect on luteinizing hormone surges [33, 34]. The brain sections obtained from these animals were subjected to immunostaining for ESR2 as well as Nissl staining, to examine ESR2<sup>+</sup> cell numbers in the anteroventral periventricular nucleus (AVPV), medial preoptic nucleus (MPN), principal nucleus of the BNST (BNSTp), posterodorsal subnucleus of the medial amygdala (MePD), supraoptic nucleus (SON), PVN, and dorsal raphe nucleus (DRN).

### General procedures

#### *Tissue preparation*

Animals were deeply anesthetized by the intraperitoneal injection of mixed anesthesia: medetomidine hydrochloride (0.3 mg/kg body weight), midazolam (4.0 mg/kg body weight), and butorphanol tartrate (5.0 mg/kg body weight). The animals were then perfused transcardially with saline followed by 4% paraformaldehyde in 0.1 M phosphate buffer (pH 7.4). The brains were postfixed with the same fixative at 4 °C overnight, immersed in 0.1 M

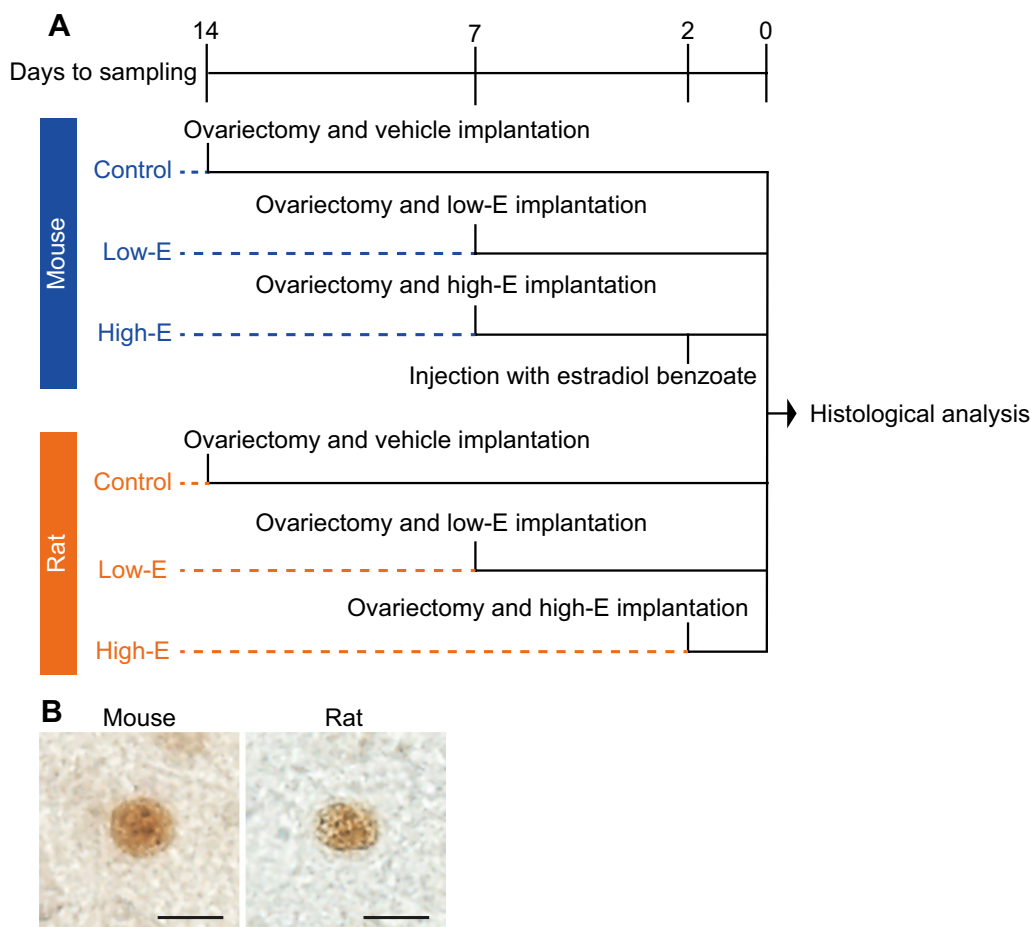


**Fig. 1** Supplement to methods. Time courses of the estrogen manipulations applied to female mice and rats (**A**). Representative photomicrographs of mouse and rat ESR2<sup>+</sup> cells with immunopositive signal in the cell nuclei (**B**). Scale bars = 10 μm

phosphate buffer containing 20% sucrose for 2–5 days at 4 °C, and then frozen in n-hexane at –80 °C. Brains were sectioned coronally using a cryostat at a thickness of 30 μm for mice and 40 μm for rats. The mouse and rat brain sections were collected at intervals of 90 μm and 160 μm, respectively, for mapping of ESR2<sup>+</sup> cells, and at intervals of 60 μm and 80 μm, respectively, for examining the effects of estrogen manipulation.

#### Characterization of the anti-ESR2 antibody

The anti-ESR2 mouse monoclonal antibody (PPZ0506, Perseus Proteomics, Tokyo, Japan; RRID:AB\_1964229), raised against amino acids 2–88 from the N-terminal of human ESR2 protein, has been confirmed to specifically recognize FLAG-tagged mouse, rat, and human ESR2 proteins using western blotting and immunocytofluorescence detection [28]. In addition, our previous studies have established its applicability to the immunohistochemical detection of mouse and rat ESR2 proteins [29, 30, 35].

#### Immunohistochemistry for ESR2 and Nissl staining

Brain sections were mounted on FRONTIER-coated glass slides (Matsunami Glass, Osaka, Japan) and warmed on a slide warmer at 60 °C for 1 h. The sections were then rinsed in distilled water and placed in methanol containing 0.3% H<sub>2</sub>O<sub>2</sub> for 5 min at room temperature. Next, they were rinsed in 0.1 M phosphate-buffered saline (PBS, pH 7.4), autoclaved at 121 °C for 10 min in citrate-based antigen unmasking solution (pH 6.0; H-3300, Vector Laboratories, Newark, CA, USA) for antigen retrieval, and rinsed again in PBS. The mouse brain sections were then blocked for 30 min at room temperature with blocking reagent (a component of the Mouse-on-Mouse Polymer IHC Kit, ab269452, Abcam, Cambridge, UK), whereas the rat brain sections were blocked for 30 min at room temperature with 5% normal goat serum in PBS containing 0.3% Triton X-100 (PBST, pH 7.4). This blocking was followed by incubation at 4 °C overnight with anti-ESR2 antibody (PPZ0506), which was dissolved in PBST (1:

2000) for the mouse brain sections and in 5% normal goat serum in PBST (1: 2000) for the rat brain sections. For the negative controls, residual brain sections from the series were exposed to solvent without the anti-ESR2 antibody. After rinsing with PBST, the mouse brain sections were incubated for 15 min at room temperature with horseradish peroxidase polymer detector reagent (a component of the Mouse-on-Mouse Polymer IHC Kit), whereas the rat brain sections were incubated for 2 h at room temperature with 50% goat anti-mouse immunoglobulin G conjugated to a horseradish peroxidase-labeled polymer (ab214879, Abcam) in PBST. All sections were then rinsed in PBS and 0.01 M Tris-HCl (pH 7.5) before the ESR2<sup>+</sup> signals were visualized using 200 µg/mL of 3,3'-diaminobenzidine tetrahydrochloride (Merck, Darmstadt, Germany) and 0.01% H<sub>2</sub>O<sub>2</sub> in 0.05 M Tris-HCl (pH 7.5). Finally, the sections were rinsed in PBS, stained with 0.025% violet solution, dehydrated through an ethanol series, cleared with xylene, and coverslipped using mounting medium (Entellan new, Merck).

#### **Immunohistochemistry for OXT or AVP + ESR2**

Mouse and rat brain sections were placed in PBST containing 0.3% H<sub>2</sub>O<sub>2</sub> for 30 min at room temperature. Next, they were rinsed in 0.1 M PBS, blocked for 30 min at room temperature with 5% normal goat serum in PBST, and then immunoreacted in 5% normal goat serum in PBST containing rabbit anti-OXT antibody (1: 20,000; AB911, Millipore, MA, USA; RRID:AB\_2157629) or guinea-pig anti-AVP antibody (1: 5000; T5048, Peninsula Laboratories, CA, USA; RRID:AB\_518680) at 4 °C overnight. After rinsing with PBST, the brain sections were incubated for 2 h at room temperature with 50% goat anti-rabbit immunoglobulin G conjugated to a horseradish peroxidase-labeled polymer (ab214880, Abcam) in PBST or horseradish peroxidase-labeled goat anti-guinea pig immunoglobulin G (SA00001-12, Proteintech, IL, USA; RRID:AB\_2890975) in PBST (1: 1000). All sections were then rinsed in PBST before the immunoreactive signals were visualized using an ImmPACT SG substrate kit (SK-4705, Vector Laboratories). After the sections were rinsed in PBST, antibodies were removed from the sections by incubation with 0.1 M of glycine-HCl buffer (pH 2.2) for 90 min at room temperature. Subsequently, OXT or AVP-immunostained sections were mounted on FRONTIER-coated glass slides, warmed on a slide warmer at 60 °C for 1 h, and subjected to ESR2 immunostaining. After ESR2 immunoreactive signals were detected, the sections were rinsed in PBS, dehydrated through an ethanol series, cleared with xylene, and coverslipped using mounting medium (Entellan new).

#### **Histological analysis**

Digital images of brain sections were obtained using a microscope (BX51, Olympus, Tokyo, Japan) equipped with a charge-coupled device camera (DP73, Olympus) and a microscope (DMD108, Leica Microsystems, Wetzlar, Germany); the same imaging conditions were used for the same animal species. Atlases of brains of mice and rats were used as references to identify brain regions [36, 37]. To examine sex differences and the effects of estrogen manipulation on ESR2 expression, photomicrographs of all brain sections containing the target regions were obtained after blinding the specimens. Target neural nuclei identified as clusters of Nissl-stained neurons were traced as outlines of the region of interest using ImageJ software (National Institutes of Health, Bethesda, MD, USA; RRID: SCR\_003070). In the regions of interest, cell nuclei with immunopositive signals (Fig. 1B) were manually counted as ESR2<sup>+</sup> cells. All paired neural nuclei were analyzed on the left side of the brain because no apparent laterality was identified. See Additional file 9: Tables S1 and Additional file 10: Table S2 for the number of brain sections used for the cell counting.

#### **Statistical analysis**

Welch's t-test was used to assess statistical differences between sexes. One-way analysis of variance was used to determine differences in data among females who had been ovariectomized and treated with estrogen. When significant effects were detected by one-way analysis of variance, Tukey-Kramer test was performed to compare experimental groups. Differences were considered significant at  $p < 0.05$ . GraphPad Prism software version 9.5 (GraphPad, San Diego, CA, USA; RRID:SCR\_002798) was used for all statistical analyses.

## **Results**

#### **Distribution of ESR2<sup>+</sup> cells in the brains of mice and rats**

Coronal brain sections were prepared from adult gonadally intact mice and rats of both sexes before being immunostained with a well-validated anti-ESR2 antibody (PPZ0506). Overall, ESR2<sup>+</sup> cells were observed in several subregions of the brain—the preoptic area, extended amygdala, hypothalamus, mesencephalon, and cerebral cortex—with similar distribution patterns between mice (Fig. 2A) and rats (Fig. 2B) of both sexes (Table 1). However, some brain subregions showed sex and/or interspecies differences in the numbers and distributions of ESR2<sup>+</sup> cells. No ESR2<sup>+</sup> cells were observed in the olfactory bulb, hippocampal formation, cerebellum, pons, or medulla oblongata in either mice or rats (Additional file 1: Fig. S1, Additional file 2: Fig. S2). When the primary antibody reaction was omitted, some neural fibers

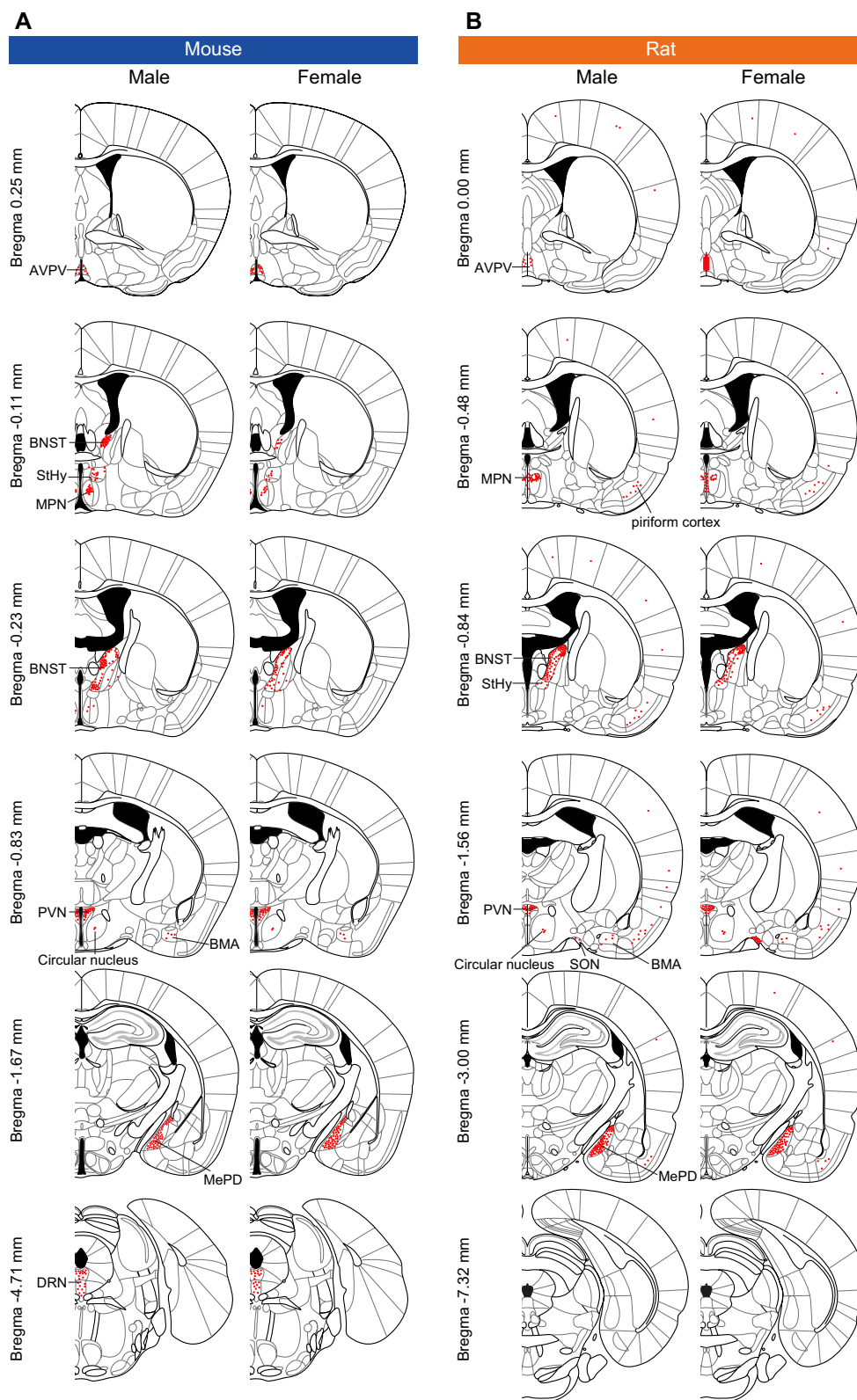


**Fig. 2** Distribution of ESR2<sup>+</sup> cells in mouse and rat brains. Schematic illustrations of ESR2<sup>+</sup> cell distributions in the brains of mice (A) and rats (B). Illustrations were drawn based on the Paxinos and Franklin mouse brain atlas [36] and the Paxinos and Watson rat brain atlas [37]. Red dots indicate sites where ESR2<sup>+</sup> cells were commonly observed in the animals in this study

**Table 1** Distribution of ESR2<sup>+</sup> cells in the brains of mice and rats

Brain regions	Mouse		Rat	
	Male	Female	Male	Female
Telencephalon				
Pallium				
Isocortex				
Piriform cortex				
Layer 4, 5	–	–	+	+
Layer 1, 2, 3, 6	–	–	–	–
Endopiriform nu	–	–	–	–
Others				
Layer 4, 5	–	–	–/+	–/+
Layer 1, 2, 3, 6	–	–	–	–
Olfactory areas				
Main olfactory bulb	–*	–*	–	–
Accessory olfactory bulb	–*	–*	–	–
Others	–	–	–	–
Hippocampal formation	–	–	–	–
Subpallium				
Clastrum	–	–	–	–
Striatum	–	–	–	–
Pallidum	–	–	–	–
Diagonal domain	–	–	–	–
Septum	–	–	–	–
Preoptic area				
Anteroventral periventricular nu	+	++	++	+++
Lateral preoptic area	–	–	–	–
Medial preoptic area	++	+	++	+
Median preoptic nu	–	–	–	–
Ventrolateral preoptic nu	–	–	–	–
Extended amygdala				
Amygdala				
Lateral amygdala nu	–	–	–	–
Basolateral amygdala nu	–	–	–	–
Basomedial amygdala nu	+	+	+	+
Posterior amygdala nu	+++	++	+++	++
Bed nu of the stria terminalis				
Lateral posterior division	++	+	++	+
Medial posterior division	+++	++	+++	++
Others	–	–	–	–
Striohypothalamic nu	+	+	+	+
Substantia innominata	–	–	–	–
Thalamus	–	–	–	–
Hypothalamus				
Periventricular hypothalamic nu	+++	+++	+++	+++
Circular nu	+	+	+	+
Supraoptic nu	–	–	–/+	++
Others	–	–	–	–
Cerebellum	–	–	–	–
Mesencephalon				
Dorsal raphe nu	++	++	–	–

**Table 1** (continued)

Brain regions	Mouse		Rat	
	Male	Female	Male	Female
Others	–	–	–	–
Rhombencephalon				
Pons	–	–	–	–
Medulla	–	–	–	–

–, no ESR2<sup>+</sup> cells; –/+ , no or a few ESR2<sup>+</sup> cells depending on the individual; +, a few ESR2<sup>+</sup> cells; ++, abundant ESR2<sup>+</sup> cells; +++, very abundant ESR2<sup>+</sup> cells; \*, non-specific-stained; nu, nucleus

in the white matter were non-specifically stained, but cell nuclei were not stained (Additional file 3: Fig. S3). In particular, mouse olfactory bulbs were darkly stained regardless of the primary antibody reaction, and cell nuclei were not stained (Additional file 1: Fig. S1).

#### Preoptic area

In the preoptic area, ESR2<sup>+</sup> cells were localized in the AVPV and MPN and sparsely distributed in their surrounding regions. There were both sex and interspecies differences in the distribution profiles of ESR2<sup>+</sup> cells in the AVPV and MPN. In mice, weakly stained ESR2<sup>+</sup> cells were distributed throughout the AVPV (Fig. 3A) and were more abundant in females ( $T_6=3.88$ ,  $p<0.01$ ; Fig. 3B). In male rats, ESR2<sup>+</sup> cells were sparsely distributed in the AVPV, similar to in male mice. In contrast, in female rats, ESR2<sup>+</sup> cells were restricted to the medial region of the AVPV, termed the rostral periventricular area of the third ventricle (Fig. 3C). Furthermore, ESR2<sup>+</sup> cells in the rat AVPV were more abundant in females than in males ( $T_6=5.71$ ,  $p<0.005$ ; Fig. 3D). In both male and female rats, the ESR2<sup>+</sup> cell population in the rostral periventricular area of the third ventricle of the AVPV was continuously distributed to the caudal side of the medial preoptic area. Moreover, in both the mouse and rat MPN, strongly stained ESR2<sup>+</sup> cells were localized in the central region (Fig. 3E, G). In the rat MPN, ESR2<sup>+</sup> cells were distributed mainly in the periphery of the Nissl-stained neuron cluster that is known as the sexually dimorphic nucleus of the preoptic area (SDN-POA). In both the mouse and rat MPN, more ESR2<sup>+</sup> cells were observed in males than in females (mouse,  $T_6=2.57$ ,  $p<0.01$ , Fig. 3F; rat,  $T_6=9.46$ ,  $p<0.0001$ , Fig. 3H).

#### Extended amygdala

In both mice and rats, ESR2<sup>+</sup> cells were observed in several subnuclei in the extended amygdala, with no apparent interspecies differences in distribution. However, there was a male-biased difference in the number of ESR2<sup>+</sup> cells in this region. In the mouse and rat BNST,

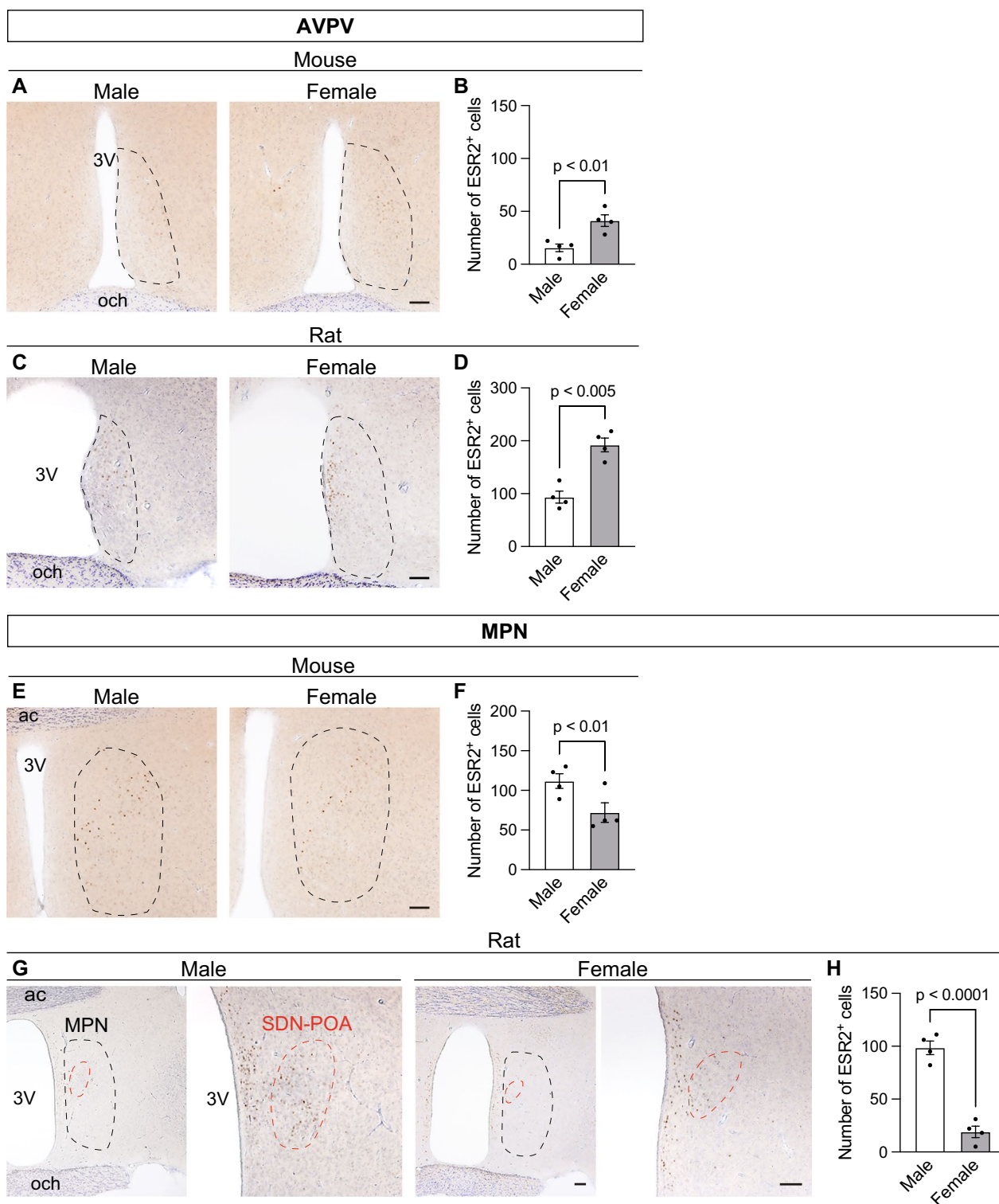


**Fig. 3** Distribution of ESR2<sup>+</sup> cells in mouse and rat preoptic areas and its sex differences. Representative photomicrographs of ESR2- and Nissl-stained brain sections containing the AVPV of mice (**A**) and rats (**C**) and the MPN of mice (**E**) and rats (**G**). The black dashed line in each panel indicates the region of interest. The right images of panel G correspond to magnified views of the SDN-POA, surrounded by a red dashed line. 3V, third ventricle; ac, anterior commissure; och, optic chiasm. Scale bars = 100 μm. The numbers of ESR2<sup>+</sup> cells in the AVPV of mice (**B**) and rats (**D**) and the MPN of mice (**F**) and rats (**H**). Data are presented as the mean ± standard error of the mean (n = 4). Black dots represent individual data

ESR2<sup>+</sup> cells were widely distributed in the posterior part, and were especially abundant in a subnucleus of the posterior medial region, known as the BNSTp (Fig. 4A, C). As in the SDN-POA, ESR2<sup>+</sup> cells were densely distributed in the periphery of the BNSTp and sparsely distributed in the center. In addition, ESR2<sup>+</sup> cells were more abundant in males than in females (mouse,  $T_6=4.07$ ,  $p<0.0005$ , Fig. 4B; rat,  $T_6=8.36$ ,  $p<0.0001$ , Fig. 4D). A few ESR2<sup>+</sup> cells were observed in the striohypothalamic nucleus (StHy), which borders the BNST and preoptic area (Figs. 2A, B). In the amygdala, ESR2<sup>+</sup> cells were diffusely distributed in and around the basomedial amygdaloid nucleus (BMA) in the anterior region (Fig. 4E, H), and were densely localized in the MePD in the posterior region (Fig. 4F, I). In the MePD, there were more ESR2<sup>+</sup> cells in males than in females (mouse,  $T_6=6.87$ ,  $p<0.05$ , Fig. 4G; rat,  $T_6=8.36$ ,  $p<0.0001$ , Fig. 4J).

### Hypothalamus

In both mice and rats, many ESR2<sup>+</sup> cells were observed in the PVN (Fig. 5A, C). In particular, ESR2<sup>+</sup> cells were densely located in the posterior and dorsolateral part of this region. There were no apparent sex or interspecies differences in ESR2<sup>+</sup> cell distribution in the PVN (Fig. 5B, D). Colocalization of ESR2/OXT and ESR2/AVP was determined by double immunostaining. Most ESR2<sup>+</sup> cells were OXT- and AVP-immunonegative in both mice and rats because OXT- and AVP-immunopositive cells were located mainly in the anterior part of the PVN (Additional file 4: Fig. S4, Additional file 5: Fig. S5). However, co-immunopositive cells were found in overlapping regions of the cell population. Among co-immunopositive cells, OXT-immunopositive ESR2<sup>+</sup> cells were more prevalently found in mice, whereas AVP-immunopositive ESR2<sup>+</sup> cells were more common in rats. In addition, a few ESR2<sup>+</sup> cells were observed in the circular nucleus—a small nucleus located between the PVN and SON—in both sexes (Fig. 5E–H). In the circular nuclei, OXT-positive ESR2<sup>+</sup> cells were more prevalent than AVP-positive ESR2<sup>+</sup> cells. (Additional file 6: Fig. S6). In the mouse hypothalamus, ESR2<sup>+</sup> cells were observed in the PVN and circular nucleus only (Fig. 5I), whereas in the rat hypothalamus, they were also observed in the SON (Fig. 5J). Although ESR2<sup>+</sup> cells were densely distributed in the female rat SON of all examined, only a few ESR2<sup>+</sup> cells were observed in one of the four specimens prepared from the male rat SON (no ESR2<sup>+</sup> cells were detected in the other three specimens from male rats). There was thus a female-biased difference in ESR2<sup>+</sup> cell number in the rat SON ( $T_6=12.38$ ,  $p<0.0001$ ; Fig. 5K). In the SON of female rats, more AVP-immunopositive ESR2<sup>+</sup> cells were found than OXT-immunopositive ESR2<sup>+</sup> cells (Additional file 7: Fig. S7).

### Mesencephalon

In mice, ESR2<sup>+</sup> cells were localized in the dorsal and ventral parts of the DRN (Fig. 6A), with no sex differences in distribution (Fig. 6B). In contrast, no ESR2<sup>+</sup> cells were observed in any rat mesencephalic regions, including the DRN (Fig. 6C).

### Cerebral cortex

A few weakly stained ESR2<sup>+</sup> cells were diffusely distributed in the rat cerebral cortex (Fig. 2B). These ESR2<sup>+</sup> cells were more abundant in the piriform cortex (5–10 cells/section) than in other areas (Fig. 6D) and were mainly localized in layers 4–5. In contrast, no ESR2<sup>+</sup> cells were observed in the mouse cerebral cortex.

### Effects of estrogen manipulation on ESR2 expression in female mice and rats

Ovariectomized female mice and rats underwent estrogen manipulation before their brains were used for immunohistochemical analysis. Overall, ESR2<sup>+</sup> cells were observed in estrogen-manipulated animals in the regions where ESR2 was detected in intact female mice and rats (Additional file 8: Fig. S8). The mouse SON and rat DRN did not express ESR2 even though estrogen milieu was manipulated.

In female mice, estrogen manipulation significantly affected ESR2<sup>+</sup> cell numbers in the AVPV ( $F_{2,12}=8.31$ ,  $p<0.01$ ; Fig. 7A), MPN ( $F_{2,12}=4.38$ ,  $p<0.05$ ; Fig. 7B), BNSTp ( $F_{2,12}=39.71$ ,  $p<0.0001$ ; Fig. 7C), MePD ( $F_{2,12}=35.15$ ,  $p<0.0001$ ; Fig. 7D), PVN ( $F_{2,12}=20.52$ ,  $p<0.0001$ ; Fig. 7F), and DRN ( $F_{2,12}=27.78$ ,  $p<0.0001$ ; Fig. 7G), but not in the SON (Fig. 7E). Low-E treatment significantly increased ESR2<sup>+</sup> cell numbers ( $p<0.05$ ) in the AVPV, MePD, and PVN compared with controls (Fig. 7A, D, F). In contrast, high-E treatment did not affect ESR2<sup>+</sup> cell number in the AVPV (Fig. 7A), but significantly decreased ESR2<sup>+</sup> cell numbers ( $p<0.05$ ) in the MPN, BNSTp, MePD, PVN, and DRN (Fig. 7B–D, E, G).

In female rats, estrogen manipulation significantly affected ESR2<sup>+</sup> cell numbers in the AVPV ( $F_{2,12}=13.72$ ,  $p<0.001$ ; Fig. 7H), MPN ( $F_{2,12}=8.76$ ,  $p<0.005$ ; Fig. 7I), BNSTp ( $F_{2,12}=15.93$ ,  $p<0.0005$ ; Fig. 7J), MePD ( $F_{2,12}=14.08$ ,  $p<0.001$ ; Fig. 7K), SON ( $F_{2,12}=5.48$ ,  $p<0.05$ ; Fig. 7L), and PVN ( $F_{2,12}=8.31$ ,  $p<0.01$ ; Fig. 7M), but not in the DRN (Fig. 7N). As in mice, low-E treatment significantly increased ESR2<sup>+</sup> cell numbers ( $p<0.05$ ) in the AVPV, BNSTp, MePD, and PVN compared with controls (Fig. 7H, J, K, M). In contrast, high-E treatment did not affect ESR2<sup>+</sup> cell numbers in the AVPV,

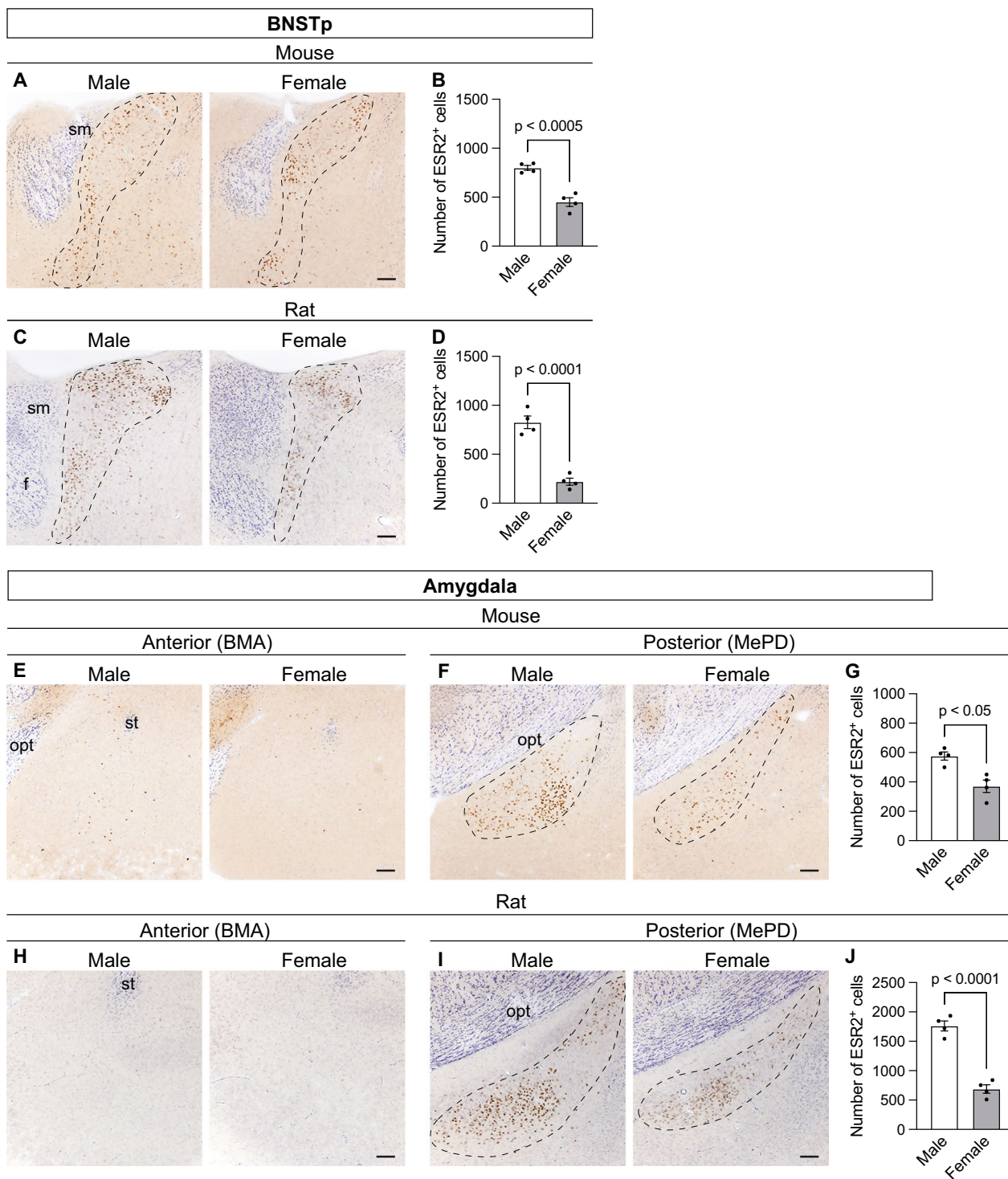


**Fig. 4** Distribution of ESR2<sup>+</sup> cells in mouse and rat extended amygdalae and its sex differences. Representative photomicrographs of ESR2- and Nissl-stained brain sections containing the BNSTp of mice (**A**) and rats (**C**) and the amygdala of mice (**E** and **F**) and rats (**H** and **I**). The dashed line in each panel indicates the region of interest. f, fornix; opt, optic tract; sm, stria medullaris; st, stria terminalis. Scale bars = 100 μm. The numbers of ESR2<sup>+</sup> cells in the BNSTp of mice (**B**) and rats (**D**) and the MePD of mice (**G**) and rats (**J**). Data are presented as the mean ± standard error of the mean (n=4). Black dots represent individual data

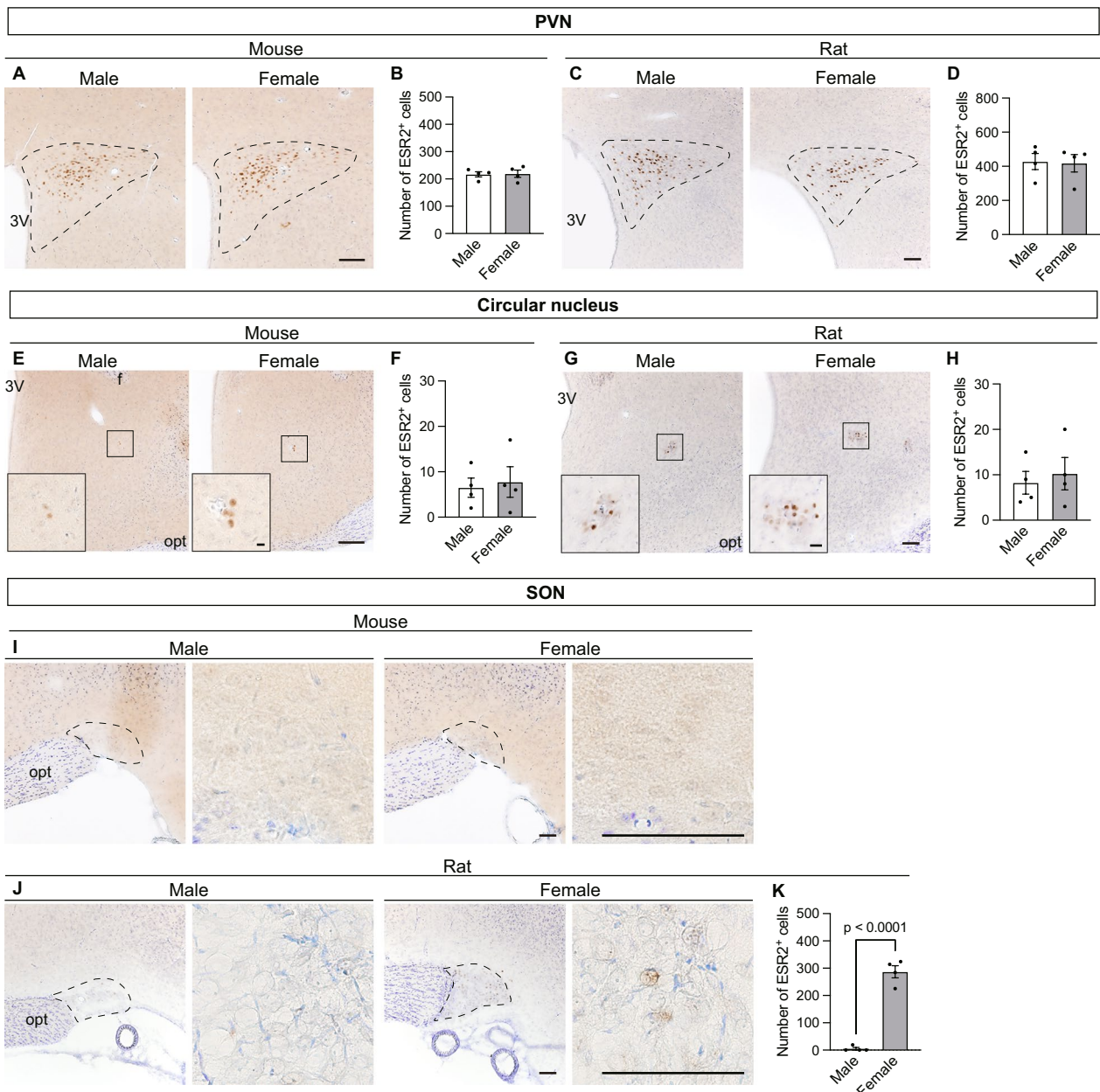


**Fig. 5** Distribution of ESR2<sup>+</sup> cells in mouse and rat hypothalami and its sex differences. Representative photomicrographs of ESR2- and Nissl-stained brain sections containing the PVN of mice (**A**) and rats (**C**), the circular nucleus of mice (**E**) and rats (**G**), and the SON of mice (**I**) and rats (**J**). The dashed line in each panel indicates the region of interest. The insets of panel **E** and **G** show high-magnification views of the circular nucleus and are indicated by the small frames. 3 V, third ventricle; f, fornix; opt, optic tract. Scale bars = 10  $\mu$ m in the inset of Panel **G** and 100  $\mu$ m in all other images. The numbers of ESR2<sup>+</sup> cells in the PVN of mice (**B**) and rats (**D**), the circular nucleus of mice (**F**) and rats (**H**), and the SON of rats (**K**). Data are presented as the mean  $\pm$  standard error of the mean ( $n = 4$ ). Black dots represent individual data

BNSTp, MePD, or PVN (Fig. 7H, J, K, M, but significantly decreased ESR2<sup>+</sup> cell numbers ( $p < 0.05$ ) in the MPN and SON (Fig. 7L, L).

## Discussion

We immunostained ESR2 proteins in mouse and rat brains of both sexes using the well-validated monoclonal antibody (PPZ0506) to determine ESR2<sup>+</sup> cell distributions. In this way, we revealed sex and interspecies differences in ESR2<sup>+</sup> cell distributions and identified

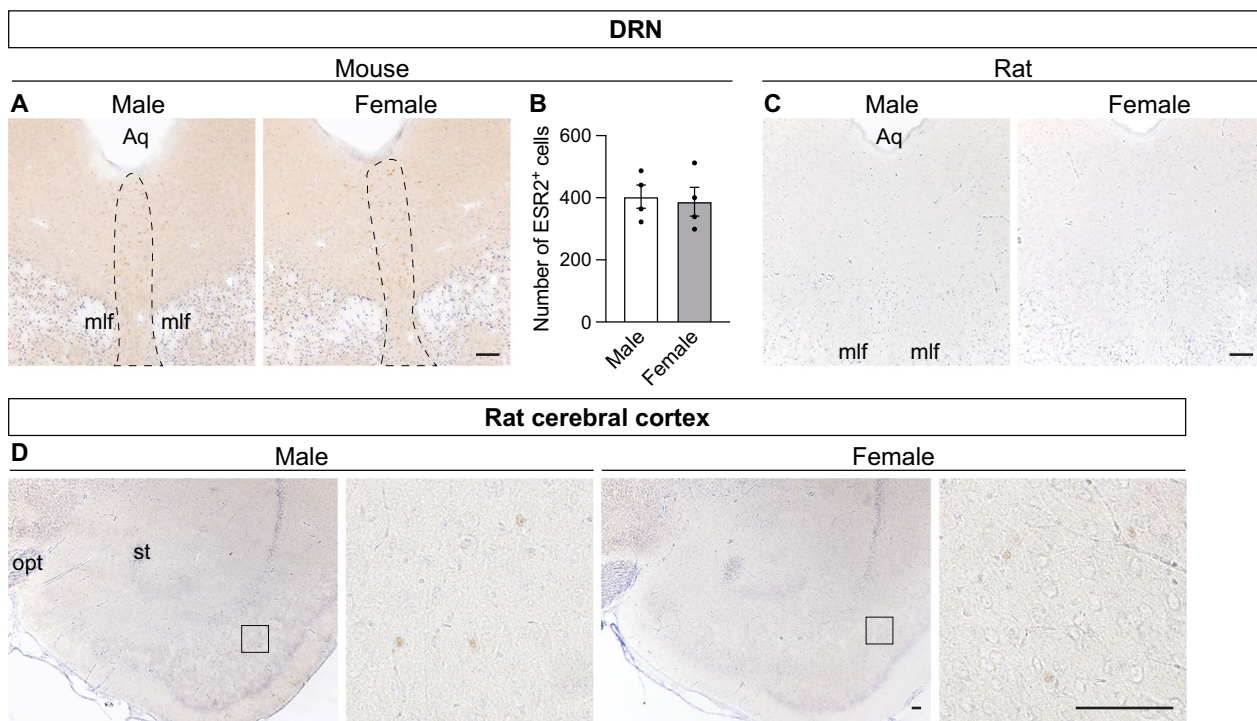


**Fig. 6** Distribution of ESR2<sup>+</sup> cells in mouse and rat mesencephalons and cerebral cortices. Representative photomicrographs of ESR2- and Nissl-stained brain sections containing the DRN of mice (**A**) and rats (**C**) and the cerebral cortex of rats (**D**). The dashed line in panel **A** indicates the region of interest. The right images of panel **D** correspond to magnified views of regions indicated by the small frames. Aq, mesencephalic aqueduct; mlf, medial longitudinal fasciculus; opt, optic tract; st, stria terminalis. Scale bars = 100  $\mu$ m. The numbers of ESR2<sup>+</sup> cells in the DRN of mice (**B**). Data are presented as the mean  $\pm$  standard error of the mean (n = 4). Black dots represent individual data

hormonal effects on their patterns in female rodent brains. The expression profiles of ESR2 in rodent brains have been a subject of great controversy, despite several attempts to study their localization. Although the details vary from report to report, previous studies using home-made or commercial antibodies have generally shown a wide distribution of ESR2 in rodent brains [17–21]. However, in situ hybridization data from the Allen brain atlas (<https://mouse.brain-map.org>) indicate that mouse *ESR2* mRNAs are expressed in a more localized manner in several brain regions, including the preoptic area, extended amygdala, hypothalamus, and mesencephalon. Considering the differences in results among the antibodies used, it is possible that previous reports of widespread ESR2 expression were overestimated due to false-positive antibody signals. Our immunohistochemical analysis using PPZ0506 revealed that ESR2 proteins are relatively localized in rodent brains, and our results are in good agreement with the expression patterns of *ESR2* mRNAs.

Sheng et al. [38] reported that ESR2 is expressed in the DRN of mice but not rats. In the present study, we found further species-related differences in immunoreactive signals in several brain regions: ESR2 staining was observed in the DRN of mice but not rats, and in

the SON and cerebral cortex of rats but not mice. Our previous study [28] confirmed the specific cross-reactivity of PPZ0506 antibody against both mouse and rat ESR2, indicating that the distinct immunoreactive signals between mice and rats are indeed because of species-related differences in ESR2 expression. Although the neurochemical characteristics of ESR2<sup>+</sup> cells in the rat cerebral cortex are unclear, it is likely that most ESR2<sup>+</sup> cells in the rat SON are AVP neurons [23], whereas those in the mouse DRN are probably serotonin neurons [24]. Co-expression of ESR2 and AVP in the female rat SON is also demonstrated in the present study. These species-dependent expression profiles suggest that ESR2 may be involved in species-related differences in the effects of estrogen on the AVP and serotonin systems, although this possibility requires further investigation. In addition, although the distribution of ESR2<sup>+</sup> cells in the PVN was not species-specific, species differences in neurochemical properties may be present, as indicated by the different abundance of AVP-immunopositive and OXT-immunopositive ESR2<sup>+</sup> cells in mice and rats. Future research is needed to characterize the neurochemistry of the ESR2<sup>+</sup> cells which were mapped in this study.

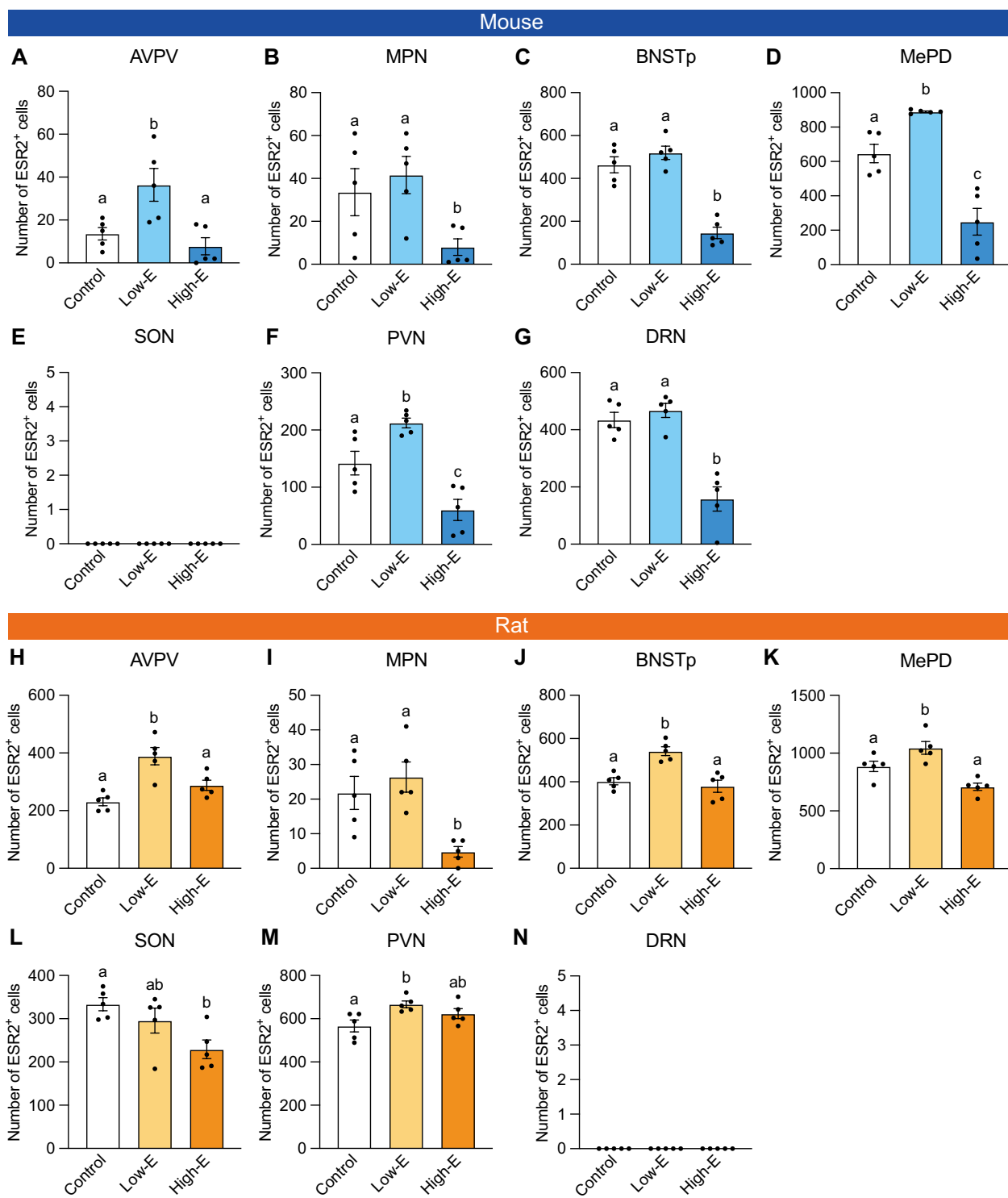


**Fig. 7** Effects of estrogen manipulation on ESR2<sup>+</sup> cell number in female mouse and rat brain subregions. The number of ESR2<sup>+</sup> cells in the AVPV (A), MPN (B), BNSTp (C), MePD (D), SON (E), PVN (F), and DRN (G) of control, low-E, and high-E female mice. The numbers of ESR2<sup>+</sup> cells in the AVPV (H), MPN (I), BNSTp (J), MePD (K), SON (L), PVN (M), and DRN (N) of control, low-E, and high-E female rats. Data are presented as the mean ± standard error of the mean (n = 5). Black dots represent individual data. Values with different letters differ significantly (p < 0.05)

In both mice and rats, the distribution profiles of ESR2<sup>+</sup> cells exhibited sex differences in several regions, most of which are known SDNs. Mouse and rat AVPVs reportedly display female-biased differences in their volumes and neuronal numbers [39, 40]. In the rat AVPV, the majority of kisspeptin neurons co-express *ESR2* mRNA [23], and there are more kisspeptin neurons in the AVPV in females than in males [41]. Furthermore, although neurons co-expressing kisspeptin and *ESR2* mRNA are scattered throughout the AVPVs of male and female mice and male rats, they are restricted to the rostral periventricular area of the third ventricle in female rats [42–44]. The species- and sex-dependent distribution profiles of ESR2<sup>+</sup> cells observed in the present study are therefore in good agreement with the reports of *ESR2* mRNA-expressing cells in previous studies. Because AVPV-specific *ESR2* knockdown induces abnormal sexual cycles [42], *ESR2* in the AVPV may regulate the reproductive axis via positive estrogen feedback provided by AVPV kisspeptin neurons. In contrast, ESR2<sup>+</sup> cells in the MPN, BNSTp, and MePD were more abundant in males than in females in the present study. Because these SDNs reportedly have male-biased differences in their volumes and neuronal numbers [45–47], the biased distributions of ESR2<sup>+</sup> cells may result from the sexually dimorphic structures of these nuclei. Moreover, in these male-biased SDNs, there are more neurons that express calbindin-D28K, androgen receptor, and/or monooxygenase DBH-like 1 in males than in females [48–51], indicating that neurons expressing these genes are candidate ESR2<sup>+</sup> cells. These SDNs (i.e., the MPN, BNSTp, and MePD) are essential for the control of social and/or anxiety-like behaviors, and their functions are modulated by estrogens in both sexes [52, 53]. The sex-dependent expression profiles of *ESR2* in these SDNs therefore suggest that *ESR2* may modulate these phenomena. To support this idea, it has been reported that *ESR2* knockdown in the medial preoptic area in the pubertal period reduces intermale aggression, and that MePD-specific *ESR2* knockdown in the adult period abolishes partner preference in male mice [54]. In addition, specific activation of BNSTp *ESR2*-expressing neurons leads to sexual satiety in male mice [55]. Notably, *ESR2* was not expressed in the mouse SON, and the rat SON exhibited a female-biased difference in *ESR2* expression. However, our previous analysis using in situ hybridization did not show any sex differences in *ESR2* mRNA expression in the rat SON [23]. Sex differences in *ESR2* expression may therefore be partly caused by post-transcriptional and/or post-translational regulation.

In the present study, *ESR2* expression in the brains of female mice and rats fluctuated in response to circulating estrogen levels. The effects of estrogen manipulation on

ESR2<sup>+</sup> cell numbers displayed similar trends in ovariectomized mice and rats: low-E treatment increased ESR2<sup>+</sup> cell numbers, whereas high-E treatment decreased them. Our estrogen manipulations mimicked distinct hormonal conditions: estrogen concentrations during low-E treatment corresponded to the blood estrogen levels that cause luteinizing hormone pulses during the diestrus phase [31, 32], and those during high-E treatment corresponded to blood estrogen levels above the physiological range that causes luteinizing hormone surges [33, 34]. Our results therefore indicate that *ESR2* expression in the brains of female mice and rats is maintained by estrogen at levels within the physiological range, and that estrogen depletion and exposure to excessive estrogen downregulate its expression. Our data on estrogen-dependent changes in *ESR2* expression are partially consistent with other studies. Several lines of evidence indicate that high-dose estrogen treatment inhibits the expression of *ESR2* mRNA and/or protein in the AVPV, MPN, BNST, MePD, PVN, and SON [56–58]. In contrast, other studies have reported that estrogen treatment does not alter *ESR2* mRNA expression in the MPN or BNST [59], and increases its expression in the PVN [24]. The partial discrepancy between our studies and those of others is presumably caused by differences in estrogen treatment. We treated ovariectomized females with two different concentrations of estrogens by implantation for days to weeks, whereas most previous studies administered estrogens via a single subcutaneous injection. Furthermore, because *ESR2* protein degradation is promoted by estradiol via the ubiquitin–proteasome system in vascular endothelial cells [60], *ESR2* expression may also be regulated at the protein level in the brain, thus possibly leading to discrepancies between *ESR2* mRNA and *ESR2* protein expression profiles. In the current study, low-E treatment did not affect ESR2<sup>+</sup> cell numbers in the mouse MPN, BNSTp, or DRN, or in the rat MPN or SON. Because steroid hormones are synthesized de novo as neurosteroids in certain brain regions, estrogen levels in these regions are higher than circulating levels; even when circulating estrogens are undetectable after ovariectomy, local estrogen levels remain high in these regions [61]. In addition, the expression of *Cyp19a1*, an estrogen synthase, is high in the BNSTp but scarce in the AVPV in adult mice [62]. Together, these lines of evidence suggest that estrogen levels differ among neural nuclei, which may have led to the observed regional differences in the effects of estrogen manipulation.

Changes in ESR2<sup>+</sup> cell numbers in response to circulating estrogen levels were insufficient to mask sexual dimorphism in the SDNs. Gonadal steroids during development have been considered essential for the sexually dimorphic formation of rodent SDNs. In the

AVPV, perinatal testicular androgens are converted to estrogens in the brain, and these estrogens induce apoptotic cell death, resulting in female-biased differences in volume and neuronal number in this region [3, 63]. Neonatal estradiol benzoate treatment has been reported to masculinize the distribution patterns of *ESR2* mRNA-expressing cells in the AVPV of female rats [42]. In contrast, perinatal estrogens produce male-biased differences by inhibiting apoptotic cell death [3, 63] in the MPN and BNSTp. Peripubertal gonadal steroids are also involved in the sexually dimorphic formation of these SDNs [64, 65]. Thus, gonadal steroids during development may produce sex differences in *ESR2*<sup>+</sup> cell numbers. Interestingly, *ESR2* knockout reportedly abolishes sex differences in the number of dopamine neurons in the AVPV [40], while studies using gene knockout and selective agonist treatment have shown that *ESR1*, but not *ESR2*, is essential for the formation of sex differences in neuronal numbers in the AVPV, MPN, and BNSTp [66–68]. The contribution of *ESR2* to the organizational effects of estrogens therefore remains controversial. Because perinatal estrogens upregulate *ESR2* expression via *ESR1* in the mouse BNSTp [69], sex differences in *ESR2* expression may occur via the influence of other sex steroid receptors. However, the mechanisms underlying the formation of sex differences in *ESR2* expression, and its role in the formation of SDNs, require further investigation.

Although the precise expression profiles of *ESR2* obtained in the present study provide useful insights, they are limited by the sensitivity of immunohistochemistry. We have previously reported that the immunoreactive signals obtained using our methods are weaker than those obtained using high-sensitivity *in situ* hybridization [30]. For example, immunoreactive signals were not detectable in some brain regions where *ESR2* mRNA expression has been reported, such as the hippocampus, lateral septum, median preoptic area, and arcuate nucleus [23, 24]. It therefore cannot be excluded that *ESR2* proteins may be present below the detection limit in regions without immunopositive signals. Future work will need to verify the expression of *ESR2* in such regions using more sensitive methods. In addition, the high-E dosing protocol for mice commonly used to induce an LH surge followed that of Bronson et al. [34], which requires an additional subcutaneous injection of estradiol benzoate in the high-E group compared to the other treatment groups. Since vehicle injections were not performed in the other treatment groups, it cannot be excluded that this difference in the protocols may have influenced the results.

## Perspectives and significance

Immunohistochemical detection using the reliable antibody PPZ0506 revealed the distributions of *ESR2*<sup>+</sup> cells in mouse and rat brains of both sexes. Our analyses demonstrated the presence of sex and interspecies differences in *ESR2*<sup>+</sup> cell distributions, suggesting that caution should be exercised when extrapolating *ESR2* data across species and sexes. Furthermore, our results indicate that *ESR2*<sup>+</sup> cell numbers in female rodent brains fluctuate in response to circulating estrogen levels. Because the precise expression profiles of *ESR2* proteins in rodent brains had not been previously described, our findings will be helpful for understanding the *ESR2*-mediated actions of estrogen in the brain.

## Supplementary Information

The online version contains supplementary material available at <https://doi.org/10.1186/s13293-023-00574-z>.

**Additional file 1: Figure S1.** *ESR2*-immunonegative regions of mouse brain. Representative photomicrographs of sections of the olfactory bulb, hippocampus, cerebellum, pons, and medulla oblongata of mice. The brain sections of male and female mice were *ESR2*-immunostained and Nissl-stained. Negative control sections were prepared by omitting the primary antibody. The lower images correspond to magnified views of regions indicated by the small frames. Scale bars = 1 mm in the upper panels and 100  $\mu$ m in the lower panels.

**Additional file 2: Figure S2.** *ESR2*-immunonegative regions of rat brain. Representative photomicrographs of sections of the olfactory bulb, hippocampus, cerebellum, pons, and medulla oblongata of rats. The brain sections of male and female rats were *ESR2*-immunostained and Nissl-stained. Negative control sections were prepared by omitting the primary antibody. Scale bars = 1 mm in the upper panels and 100  $\mu$ m in the lower panels.

**Additional file 3: Figure S3.** Representative photomicrographs of mouse and rat brain tissues without primary antibody during the staining process. Dashed lines indicate the BNSTp, identified as clusters of Nissl-stained neurons. f, fornix; sm, stria medullaris. Scale bars = 100  $\mu$ m.

**Additional file 4: Figure S4.** Cellular co-localization of *ESR2* and OXT or AVP in the mouse PVN. Representative photomicrographs of *ESR2*- (brown) and OXT- (blue-gray) immunostained brain sections containing the PVN of males (A) and females (B). Representative photomicrographs of *ESR2*- (brown) and AVP- (blue-gray) immunostained brain sections containing the PVN of males (C) and females (D). The lower images correspond to magnified views of regions indicated by the small frames. Scale bars = 100  $\mu$ m in the upper panels and 50  $\mu$ m in the lower panels.

**Additional file 5: Figure S5.** Cellular co-localization of *ESR2* and OXT or AVP in the rat PVN. Representative photomicrographs of *ESR2*- (brown) and OXT- (blue-gray) immunostained brain sections containing the PVN of males (A) and females (B). Representative photomicrographs of *ESR2*- (brown) and AVP- (blue-gray) immunostained brain sections containing the PVN of males (C) and females (D). The lower images correspond to magnified views of regions indicated by the small frames. Scale bars = 100  $\mu$ m in the upper panels and 50  $\mu$ m in the lower panels.

**Additional file 6: Figure S6.** Cellular co-localization of *ESR2* and OXT or AVP in the circular nucleus of mice and rats. Representative photomicrographs of *ESR2*- (brown) and OXT- (blue-gray) immunostained brain sections containing the circular nucleus of mice (A) and rats (C). Representative photomicrographs of *ESR2*- (brown) and AVP- (blue-gray) immunostained brain sections containing the circular nucleus of mice (B) and rats (D). Scale bars = 50  $\mu$ m.

**Additional file 7: Figure S7.** Cellular co-localization of ESR2 and OXT or AVP in the female rat SON. Representative photomicrographs of ESR2- (brown) and OXT- (blue-gray) immunostained brain sections containing the SON of female rats (A). Representative photomicrographs of ESR2- (brown) and AVP- (blue-gray) immunostained brain sections containing the SON of female rats (B). The right images correspond to magnified views of regions indicated by the small frames. Scale bars = 100  $\mu$ m in the left panels and 50  $\mu$ m in the right panels.

**Additional file 8: Figure S8.** Representative photomicrographs of immunostained brain sections of estrogen-manipulated female mice and rats. Representative photomicrographs of ESR2- and Nissl-stained brain sections containing the AVPV, MPN, BNSTp, MePD, SON, PVN, and DRN of female mice and rats with control, low-E, and high-E. Scale bars = 100  $\mu$ m.

**Additional file 9: Table S1.** The number of brain sections of intact mice and rats used for ESR2<sup>+</sup> cell counting.

**Additional file 10: Table S2.** The number of brain sections of estrogen-manipulated mice and rats used for ESR2<sup>+</sup> cell counting.

### Acknowledgements

We thank Bronwen Gardner, Ph.D., from Edanz (<https://jp.edanz.com/ac>) for editing a draft of this manuscript.

### Author contributions

MM performed all experiments and was a major contributor in writing the manuscript. SH, KI, and HI advised on experimental plans and the manuscript. All authors read and approved the final manuscript.

### Funding

This work was supported by KAKENHI Grants-in-Aid (Grant Nos. 21K20659 and 23K14439 [MM] and 23K06350 [HI]).

### Availability of data and materials

The datasets analyzed during the current study are available from the corresponding author on reasonable request.

### Declarations

#### Ethics approval and consent to participate

All experiments were approved by the Nippon Medical School Animal Care and Use Committee (approval number: 2020-032) and conducted in compliance with institutional guidelines.

#### Consent for publication

Not applicable.

#### Competing interests

The authors declare that they have no competing interests.

#### Author details

<sup>1</sup>Department of Anatomy and Neurobiology, Graduate School of Medicine, Nippon Medical School, 1-1-5 Sendagi, Bunkyo-ku, Tokyo 113-8602, Japan.

Received: 7 July 2023 Accepted: 7 December 2023

Published online: 18 December 2023

### References

- Jensen EV, DeSombre ER. Estrogen-receptor interaction. *Science*. 1973;182(4108):126–34. <https://doi.org/10.1126/science.182.4108.126>.
- Kuiper GG, Enmark E, Peltö-Huikko M, Nilsson S, Gustafsson JA. Cloning of a novel receptor expressed in rat prostate and ovary. *Proc Natl Acad Sci U S A*. 1996;93(12):5925–30. <https://doi.org/10.1073/pnas.93.12.5925>.
- Tsukahara S, Morishita M. Sexually dimorphic formation of the preoptic area and the bed nucleus of the stria terminalis by neuroestrogens. *Front Neurosci*. 2020;14:797. <https://doi.org/10.3389/fnins.2020.00797>.
- Wintermantel TM, Campbell RE, Porteous R, Bock D, Grone HJ, Todman MG, et al. Definition of estrogen receptor pathway critical for estrogen positive feedback to gonadotropin-releasing hormone neurons and fertility. *Neuron*. 2006;52(2):271–80. <https://doi.org/10.1016/j.neuron.2006.07.023>.
- Yeo SH, Herbison AE. Estrogen-negative feedback and estrous cyclicity are critically dependent upon estrogen receptor- $\alpha$  expression in the arcuate nucleus of adult female mice. *Endocrinology*. 2014;155(8):2986–95. <https://doi.org/10.1210/en.2014-1128>.
- Geary N, Asarian L, Korach KS, Pfaff DW, Ogawa S. Deficits in E2-dependent control of feeding, weight gain, and cholecystokinin satiation in ER- $\alpha$  null mice. *Endocrinology*. 2001;142(11):4751–7. <https://doi.org/10.1210/endo.142.11.8504>.
- Harris HA, Katzenellenbogen JA, Katzenellenbogen BS. Characterization of the biological roles of the estrogen receptors, ER $\alpha$  and ER $\beta$ , in estrogen target tissues in vivo through the use of an ER $\alpha$ -selective ligand. *Endocrinology*. 2002;143(11):4172–7. <https://doi.org/10.1210/en.2002-220403>.
- Ogawa S, Chester AE, Hewitt SC, Walker VR, Gustafsson JA, Smithies O, et al. Abolition of male sexual behaviors in mice lacking estrogen receptors  $\alpha$  and  $\beta$  (alpha beta ERKO). *Proc Natl Acad Sci U S A*. 2000;97(26):14737–41. <https://doi.org/10.1073/pnas.250473597>.
- Trouillet AC, Ducrocq S, Naule L, Capela D, Parmentier C, Radovick S, et al. Deletion of neural estrogen receptor  $\alpha$  induces sex differential effects on reproductive behavior in mice. *Commun Biol*. 2022;5(1):383. <https://doi.org/10.1038/s42003-022-03324-w>.
- Krege JH, Hodgin JB, Couse JF, Enmark E, Warner M, Mahler JF, et al. Generation and reproductive phenotypes of mice lacking estrogen receptor  $\beta$ . *Proc Natl Acad Sci U S A*. 1998;95(26):15677–82. <https://doi.org/10.1073/pnas.95.26.15677>.
- Dombret C, Naule L, Trouillet AC, Parmentier C, Hardin-Pouzet H, Mhaouty-Kodja S. Effects of neural estrogen receptor  $\beta$  deletion on social and mood-related behaviors and underlying mechanisms in male mice. *Sci Rep*. 2020;10(1):6242. <https://doi.org/10.1038/s41598-020-63427-4>.
- Liu F, Day M, Muniz LC, Bitran D, Arias R, Revilla-Sanchez R, et al. Activation of estrogen receptor- $\beta$  regulates hippocampal synaptic plasticity and improves memory. *Nat Neurosci*. 2008;11(3):334–43. <https://doi.org/10.1038/nn2057>.
- Imwalle DB, Gustafsson JA, Rissman EF. Lack of functional estrogen receptor  $\beta$  influences anxiety behavior and serotonin content in female mice. *Physiol Behav*. 2005;84(1):157–63. <https://doi.org/10.1016/j.physbeh.2004.11.002>.
- Leite C, Madeira MD, Sa SI. Effects of sex steroids and estrogen receptor agonists on the expression of estrogen receptor  $\alpha$  in the principal division of the bed nucleus of the stria terminalis of female rats. *Brain Res*. 2014;1582:99–106. <https://doi.org/10.1016/j.brainres.2014.07.041>.
- Funabashi T, Kleopoulou SP, Brooks PJ, Kimura F, Pfaff DW, Shinohara K, et al. Changes in estrogenic regulation of estrogen receptor  $\alpha$  mRNA and progesterone receptor mRNA in the female rat hypothalamus during aging: an in situ hybridization study. *Neurosci Res*. 2000;38(1):85–92. [https://doi.org/10.1016/S0168-0102\(00\)00150-4](https://doi.org/10.1016/S0168-0102(00)00150-4).
- Arteaga-Lopez PR, Dominguez R, Cerbon MA, Mendoza-Rodriguez CA, Cruz ME. Differential mRNA expression of  $\alpha$  and  $\beta$  estrogen receptor isoforms and GnRH in the left and right side of the preoptic and anterior hypothalamic area during the estrous cycle of the rat. *Endocrine*. 2003;21(3):251–60. <https://doi.org/10.1385/ENDO.21:3:251>.
- Merchenthaler I, Lane MV, Numan S, Dellovalle TL. Distribution of estrogen receptor  $\alpha$  and  $\beta$  in the mouse central nervous system: in vivo autoradiographic and immunocytochemical analyses. *J Comp Neurol*. 2004;473(2):270–91. <https://doi.org/10.1002/cne.20128>.
- Mitra SW, Hoskin E, Yudkovitz J, Pear L, Wilkinson HA, Hayashi S, et al. Immunolocalization of estrogen receptor  $\beta$  in the mouse brain: comparison with estrogen receptor  $\alpha$ . *Endocrinology*. 2003;144(5):2055–67. <https://doi.org/10.1210/en.2002-221069>.
- Zhang JQ, Cai WQ, Zhou DS, Su BY. Distribution and differences of estrogen receptor  $\beta$  immunoreactivity in the brain of adult male and female rats. *Brain Res*. 2002;935(1–2):73–80. [https://doi.org/10.1016/S0006-8993\(02\)02460-5](https://doi.org/10.1016/S0006-8993(02)02460-5).
- Perez SE, Chen EY, Mufson EJ. Distribution of estrogen receptor  $\alpha$  and  $\beta$  immunoreactive profiles in the postnatal rat brain. *Brain Res Dev*

- Brain Res. 2003;145(1):117–39. [https://doi.org/10.1016/s0165-3806\(03\)00223-2](https://doi.org/10.1016/s0165-3806(03)00223-2).
21. Shughrue PJ, Merchenthaler I. Distribution of estrogen receptor beta immunoreactivity in the rat central nervous system. *J Comp Neurol.* 2001;436(1):64–81.
  22. Shughrue PJ, Lane MV, Merchenthaler I. Comparative distribution of estrogen receptor-alpha and -beta mRNA in the rat central nervous system. *J Comp Neurol.* 1997;388(4):507–25. [https://doi.org/10.1002/\(sici\)1096-9861\(19971201\)388:4%3c507::aid-cne1%3e3.0.co;2-6](https://doi.org/10.1002/(sici)1096-9861(19971201)388:4%3c507::aid-cne1%3e3.0.co;2-6).
  23. Kanaya M, Higo S, Ozawa H. Neurochemical characterization of neurons expressing estrogen receptor beta in the hypothalamic nuclei of rats using in situ hybridization and immunofluorescence. *Int J Mol Sci.* 2019;21:1. <https://doi.org/10.3390/ijms21010115>.
  24. Sagoshi S, Maejima S, Morishita M, Takenawa S, Otubo A, Takahashi K, et al. Detection and characterization of estrogen receptor beta expression in the brain with newly developed transgenic mice. *Neuroscience.* 2020;438:182–97. <https://doi.org/10.1016/j.neuroscience.2020.04.047>.
  25. Milner TA, Thompson LI, Wang G, Kievits JA, Martin E, Zhou P, et al. Distribution of estrogen receptor beta containing cells in the brains of bacterial artificial chromosome transgenic mice. *Brain Res.* 2010;1351:74–96. <https://doi.org/10.1016/j.brainres.2010.06.038>.
  26. Oyola MG, Thompson MK, Handa AZ, Handa RJ. Distribution and chemical composition of estrogen receptor beta neurons in the paraventricular nucleus of the female and male mouse hypothalamus. *J Comp Neurol.* 2017;525(17):3666–82. <https://doi.org/10.1002/cne.24295>.
  27. Andersson S, Sundberg M, Pristovsek N, Ibrahim A, Jonsson P, Katona B, et al. Insufficient antibody validation challenges oestrogen receptor beta research. *Nat Commun.* 2017;8:15840. <https://doi.org/10.1038/ncomms15840>.
  28. Ishii H, Otsuka M, Kanaya M, Higo S, Hattori Y, Ozawa H. Applicability of anti-human estrogen receptor beta antibody PPZ0506 for the immunodetection of rodent estrogen receptor beta proteins. *Int J Mol Sci.* 2019;20:24. <https://doi.org/10.3390/ijms20246312>.
  29. Hattori Y, Ishii H, Higo S, Otsuka M, Kanaya M, Matsumoto K, et al. Optimization of immunohistochemical detection of rat ESR2 proteins with well-validated monoclonal antibody PPZ0506. *Mol Cell Endocrinol.* 2021;523:111145. <https://doi.org/10.1016/j.mce.2020.111145>.
  30. Ozawa M, Hattori Y, Higo S, Otsuka M, Matsumoto K, Ozawa H, et al. Optimized mouse-on-mouse immunohistochemical detection of mouse ESR2 proteins with PPZ0506 monoclonal antibody. *Acta Histochem Cytochem.* 2022;55(5):159–68. <https://doi.org/10.1267/ahc.22-00043>.
  31. Porteous R, Haden P, Hackwell ECR, Singline A, Herde MK, Desai R, et al. Reformulation of PULSAR for analysis of pulsatile lh secretion and a revised model of estrogen-negative feedback in mice. *Endocrinology.* 2021;162:11. <https://doi.org/10.1210/endo.2021.00474>.
  32. Czielesky K, Prescott M, Porteous R, Campos P, Clarkson J, Steyn FJ, et al. Pulse and surge profiles of luteinizing hormone secretion in the mouse. *Endocrinology.* 2016;157(12):4794–802. <https://doi.org/10.1210/en.2016-1351>.
  33. Tsukamura H, Maeda KI, Yokoyama A. Effect of the suckling stimulus on daily LH surges induced by chronic oestrogen treatment in ovariectomized lactating rats. *J Endocrinol.* 1988;118(2):311–6. <https://doi.org/10.1677/joe.0.1180311>.
  34. Bronson FH. The regulation of luteinizing hormone secretion by estrogen: relationships among negative feedback, surge potential, and male stimulation in juvenile, peripubertal, and adult female mice. *Endocrinology.* 1981;108(2):506–16. <https://doi.org/10.1210/endo-108-2-506>.
  35. Morishita M, Higo S, Hattori Y, Ozawa M, Otsuka M, Matsumoto K, et al. Immunohistochemistry for ESR2 with a mouse monoclonal antibody (PPZ0506). *J Nippon Med Sch.* 2023. [https://doi.org/10.1272/jnms.JNMS.2023\\_90-209](https://doi.org/10.1272/jnms.JNMS.2023_90-209).
  36. Paxinos G, Franklin KB. Paxinos and Franklin's the mouse brain in stereotaxic coordinates. Cambridge: Academic press; 2019.
  37. Paxinos G, Watson C. The rat brain in stereotaxic coordinates: hard cover edition. Amsterdam: Elsevier; 2006.
  38. Sheng Z, Kawano J, Yanai A, Fujinaga R, Tanaka M, Watanabe Y, et al. Expression of estrogen receptors (alpha, beta) and androgen receptor in serotonin neurons of the rat and mouse dorsal raphe nuclei; sex and species differences. *Neurosci Res.* 2004;49(2):185–96. <https://doi.org/10.1016/j.neures.2004.02.011>.
  39. Simerly RB, Zee MC, Pendleton JW, Lubahn DB, Korach KS. Estrogen receptor-dependent sexual differentiation of dopaminergic neurons in the preoptic region of the mouse. *Proc Natl Acad Sci U S A.* 1997;94(25):14077–82. <https://doi.org/10.1073/pnas.94.25.14077>.
  40. Bodo C, Kudwa AE, Rissman EF. Both estrogen receptor-alpha and -beta are required for sexual differentiation of the anteroventral periventricular area in mice. *Endocrinology.* 2006;147(1):415–20. <https://doi.org/10.1210/en.2005-0834>.
  41. Clarkson J, Herbison AE. Postnatal development of kisspeptin neurons in mouse hypothalamus; sexual dimorphism and projections to gonadotropin-releasing hormone neurons. *Endocrinology.* 2006;147(12):5817–25. <https://doi.org/10.1210/en.2006-0787>.
  42. Orikasa C, Kondo Y, Hayashi S, McEwen BS, Sakuma Y. Sexually dimorphic expression of estrogen receptor beta in the anteroventral periventricular nucleus of the rat preoptic area: implication in luteinizing hormone surge. *Proc Natl Acad Sci U S A.* 2002;99(5):3306–11. <https://doi.org/10.1073/pnas.052707299>.
  43. Smith JT, Cunningham MJ, Rissman EF, Clifton DK, Steiner RA. Regulation of Kiss1 gene expression in the brain of the female mouse. *Endocrinology.* 2005;146(9):3686–92. <https://doi.org/10.1210/en.2005-0488>.
  44. Smith JT, Dungan HM, Stoll EA, Gottsch ML, Braun RE, Eacker SM, et al. Differential regulation of KISS-1 mRNA expression by sex steroids in the brain of the male mouse. *Endocrinology.* 2005;146(7):2976–84. <https://doi.org/10.1210/en.2005-0323>.
  45. Gorski RA, Gordon JH, Shryne JE, Southam AM. Evidence for a morphological sex difference within the medial preoptic area of the rat brain. *Brain Res.* 1978;148(2):333–46. [https://doi.org/10.1016/0006-8993\(78\)90723-0](https://doi.org/10.1016/0006-8993(78)90723-0).
  46. Hines M, Davis FC, Coquelin A, Goy RW, Gorski RA. Sexually dimorphic regions in the medial preoptic area and the bed nucleus of the stria terminalis of the guinea pig brain: a description and an investigation of their relationship to gonadal steroids in adulthood. *J Neurosci.* 1985;5(1):40–7. <https://doi.org/10.1523/JNEUROSCI.05-01-00040.1985>.
  47. Cooke BM, Tabibnia G, Breedlove SM. A brain sexual dimorphism controlled by adult circulating androgens. *Proc Natl Acad Sci U S A.* 1999;96(13):7538–40. <https://doi.org/10.1073/pnas.96.13.7538>.
  48. Orikasa C, Sakuma Y. Estrogen configures sexual dimorphism in the preoptic area of C57BL/6J and ddN strains of mice. *J Comp Neurol.* 2010;518(17):3618–29. <https://doi.org/10.1002/cne.22419>.
  49. Sickel MJ, McCarthy MM. Calbindin-D28k immunoreactivity is a marker for a subdivision of the sexually dimorphic nucleus of the preoptic area of the rat: developmental profile and gonadal steroid modulation. *J Neuroendocrinol.* 2000;12(5):397–402. <https://doi.org/10.1046/j.1365-2826.2000.00474.x>.
  50. Tsuneoka Y, Tsukahara S, Yoshida S, Takase K, Oda S, Kuroda M, et al. Moxd1 is a marker for sexual dimorphism in the medial preoptic area, bed nucleus of the stria terminalis and medial amygdala. *Front Neuroanat.* 2017;11:26. <https://doi.org/10.3389/fnana.2017.00026>.
  51. Juntti SA, Tollkuhn J, Wu MV, Fraser EJ, Soderborg T, Tan S, et al. The androgen receptor governs the execution, but not programming, of male sexual and territorial behaviors. *Neuron.* 2010;66(2):260–72. <https://doi.org/10.1016/j.neuron.2010.03.024>.
  52. Chen P, Hong W. Neural circuit mechanisms of social behavior. *Neuron.* 2018;98(1):16–30. <https://doi.org/10.1016/j.neuron.2018.02.026>.
  53. Ahrens S, Wu MV, Furlan A, Hwang GR, Paik R, Li H, et al. A central extended amygdala circuit that modulates anxiety. *J Neurosci.* 2018;38(24):5567–83. <https://doi.org/10.1523/JNEUROSCI.0705-18.2018>.
  54. Nakata M, Sano K, Musatov S, Yamaguchi N, Sakamoto T, Ogawa S. Effects of prepubertal or adult site-specific knockdown of estrogen receptor beta in the medial preoptic area and medial amygdala on social behaviors in male mice. *eNeuro.* 2016;3:2. <https://doi.org/10.1523/ENEURO.0155-15.2016>.
  55. Zhou X, Li A, Mi X, Li Y, Ding Z, An M, et al. Hyperexcited limbic neurons represent sexual satiety and reduce mating motivation. *Science.* 2023;379(6634):820–5. <https://doi.org/10.1126/science.abl4038>.
  56. Suzuki S, Handa RJ. Regulation of estrogen receptor-beta expression in the female rat hypothalamus: differential effects of dexamethasone and estradiol. *Endocrinology.* 2004;145(8):3658–70. <https://doi.org/10.1210/en.2003-1688>.
  57. Greco B, Allegretto EA, Tetel MJ, Blaustein JD. Coexpression of ER beta with ER alpha and progesterin receptor proteins in the female rat forebrain.

- effects of estradiol treatment. *Endocrinology*. 2001;142(12):5172–81. <https://doi.org/10.1210/endo.142.12.8560>.
58. Nomura M, Korach KS, Pfaff DW, Ogawa S. Estrogen receptor beta (ERbeta) protein levels in neurons depend on estrogen receptor alpha (ERalpha) gene expression and on its ligand in a brain region-specific manner. *Brain Res Mol Brain Res*. 2003;110(1):7–14. [https://doi.org/10.1016/s0169-328x\(02\)00544-2](https://doi.org/10.1016/s0169-328x(02)00544-2).
59. Patisaul HB, Whitten PL, Young LJ. Regulation of estrogen receptor beta mRNA in the brain: opposite effects of 17beta-estradiol and the phytoestrogen, coumestrol. *Brain Res Mol Brain Res*. 1999;67(1):165–71. [https://doi.org/10.1016/s0169-328x\(99\)00058-3](https://doi.org/10.1016/s0169-328x(99)00058-3).
60. Tschugguel W, Dietrich W, Zhegu Z, Stonek F, Kolbus A, Huber JC. Differential regulation of proteasome-dependent estrogen receptor alpha and beta turnover in cultured human uterine artery endothelial cells. *J Clin Endocrinol Metab*. 2003;88(5):2281–7. <https://doi.org/10.1210/jc.2002-021165>.
61. Li J, Gibbs RB. Detection of estradiol in rat brain tissues: contribution of local versus systemic production. *Psychoneuroendocrinology*. 2019;102:84–94. <https://doi.org/10.1016/j.psychneuen.2018.11.037>.
62. Kanaya M, Morishita M, Tsukahara S. Temporal expression patterns of genes related to sex steroid action in sexually dimorphic nuclei during puberty. *Front Endocrinol (Lausanne)*. 2018;9:213. <https://doi.org/10.3389/fendo.2018.00213>.
63. Ogawa S, Tsukahara S, Choleris E, Vasudevan N. Estrogenic regulation of social behavior and sexually dimorphic brain formation. *Neurosci Biobehav Rev*. 2020;110:46–59. <https://doi.org/10.1016/j.neubiorev.2018.10.012>.
64. Ahmed EI, Zehr JL, Schulz KM, Lorenz BH, DonCarlos LL, Sisk CL. Pubertal hormones modulate the addition of new cells to sexually dimorphic brain regions. *Nat Neurosci*. 2008;11(9):995–7. <https://doi.org/10.1038/nn.2178>.
65. Morishita M, Koiso R, Tsukahara S. Actions of peripubertal gonadal steroids in the formation of sexually dimorphic brain regions in mice. *Endocrinology*. 2020;161:6. <https://doi.org/10.1210/endo/bqaa063>.
66. Kanaya M, Tsuda MC, Sagoshi S, Nagata K, Morimoto C, Thu CK, et al. Regional difference in sex steroid action on formation of morphological sex differences in the anteroventral periventricular nucleus and principal nucleus of the bed nucleus of the stria terminalis. *PLoS ONE*. 2014;9(11):e112616. <https://doi.org/10.1371/journal.pone.0112616>.
67. Tsukahara S, Tsuda MC, Kurihara R, Kato Y, Kuroda Y, Nakata M, et al. Effects of aromatase or estrogen receptor gene deletion on masculinization of the principal nucleus of the bed nucleus of the stria terminalis of mice. *Neuroendocrinology*. 2011;94(2):137–47. <https://doi.org/10.1159/000327541>.
68. Lund TD, Rovis T, Chung WC, Handa RJ. Novel actions of estrogen receptor-beta on anxiety-related behaviors. *Endocrinology*. 2005;146(2):797–807. <https://doi.org/10.1210/en.2004-1158>.
69. Gegenhuber B, Wu MV, Bronstein R, Tollkuhn J. Gene regulation by gonadal hormone receptors underlies brain sex differences. *Nature*. 2022;606(7912):153–9. <https://doi.org/10.1038/s41586-022-04686-1>.

## Publisher's Note

Springer Nature remains neutral with regard to jurisdictional claims in published maps and institutional affiliations.

Ready to submit your research? Choose BMC and benefit from:

- fast, convenient online submission
- thorough peer review by experienced researchers in your field
- rapid publication on acceptance
- support for research data, including large and complex data types
- gold Open Access which fosters wider collaboration and increased citations
- maximum visibility for your research: over 100M website views per year

At BMC, research is always in progress.

Learn more [biomedcentral.com/submissions](https://biomedcentral.com/submissions)

